Lead-Chalcogenide Colloidal-Quantum-Dot Solids

Balazs, Daniel M.; Loi, Maria Antonietta

IMPORTANT NOTE: You are advised to consult the publisher's version (publisher's PDF) if you wish to cite from it. Please check the document version below.

Document Version
Publisher's PDF, also known as Version of record

[Link to publication in University of Groningen/UMCG research database](#)

Lead-Chalcogenide Colloidal-Quantum-Dot Solids: Novel Assembly Methods, Electronic Structure Control, and Application Prospects

Daniel M. Balazs and Maria Antonietta Loi*

The quest for novel semiconductors with easy, cheap fabrication and tailorable properties has led to the development of several classes of materials, such as semiconducting polymers, carbon nanotubes, hybrid perovskites, and colloidal quantum dots. All these candidates can be processed from the liquid phase, enabling easy fabrication, and are suitable for different electronic and optoelectronic applications. Here, recent developments in the field of colloidal-quantum-dot solids are discussed, with a focus on lead-chalcogenide systems. These include novel deposition methods; the recent growing understanding of their fundamental properties, driven by major successes in the control of the nanostructured assembly and surface chemistry; and selected reports on lab-scale devices showing the technological prospects of these fascinating class of materials.

1. Introduction

Colloidal quantum dots (CQDs) are semiconductor crystals in the size range of few nanometers. Due to the small size, they exhibit size-dependent optical and electronic properties through the quantum confinement effect. Moreover, CQDs in proximity interact and experience electronic coupling that depends on their distance and on the properties of the surrounding medium. These features allow for easy control of the electronic properties that could be exploited in energy harvesting and electronics applications such as transistors and more complex logic circuits, photodetectors, solar cells, and thermoelectric cells.[1–4] Alternatively, even without exploiting the size-dependent effects, the possibility of nanoscale engineering of the composition and crystallinity qualifies CQDs as excellent building blocks for bottom-up fabrication of bulk materials.[5]

Dr. D. M. Balazs, Prof. M. A. Loi
Zernike Institute for Advanced Materials
University of Groningen
Nijenborgh 4, 9747AG Groningen, The Netherlands
E-mail: m.a.loi@rug.nl

Colloidal particles are formed and stabilized by surrounding the core with a surfactant shell that keeps the CQDs isolated and prevents charge transport though the arrays.[6] Replacing this shell by shorter molecules, so-called ligands, decreases the interparticle distance and increases the electronic coupling. This is thus a crucial step in forming conductive, practically relevant assemblies.

Most early studies relied on a repetitive, layer-by-layer deposition and ligand exchange of CQDs to achieve thick conductive films, a method that resulted in the demonstration of field effect transistors and solar cells of noteworthy performances.[7–15] However, this technique only allows for limited control of the nanostructure and is not suitable for upscaling. The last few years brought several improvements in controlling the properties of CQD thin films with focus on both applications and the underlying science.[16,17] Current solar cells and transistors based on CQD arrays are on par with or better than the semiconducting polymer-based devices, showing the true prospects of these materials.[18–20]

The most interesting feature of CQD solids is their enormous specific surface area; around one third of the atoms of a few nanometer CQDs are located at the surface, experiencing lower coordination than in bulk. Changing the dielectric or chemical environment thus has a significant effect on the overall properties. Much research has been conducted into this direction as well, leading to the ability to design the properties for applications.

Here, we aim to show the most recent developments, put these results in perspective, and identify the limiting factors that limit further improvement in device performance. We focus on lead chalcogenides as they have been the subject of a variety of approaches to form solids, mainly because of their prospects in solar cell applications. However, the fundamental findings reported are valid for CQDs in general, and most methods can be used for other types of semiconductor nanocrystals as well. Although, numerous studies discuss the unique optical properties of CQDs, we have chosen to avoid their discussion here to be able to focus on the fabrication, electronic properties, and applications of CQD assemblies. In Section 2, two novel directions in sample fabrication of lead-chalcogenide CQD assemblies are discussed. The first one, the solution-phase ligand exchange, is relevant for mass production of devices, while the other, the self-assembly, is important for creating arrays with controlled nanostructure and order. Related to the difference in

order between the resulting films, the possibility of band transport in superlattices of confined CQDs is discussed, followed by the evaluation and redefinition of the criteria used to prove the transport mechanism. Section 3 discusses the advances in controlling the electronic properties using the large surface area of the CQDs, in comparison with the possibilities in bulk semiconductors. In Section 4, we give an overview on the recent developments of CQD-based energy-harvesting and electronic devices, based on either sintered or confined CQD arrays.

2. Assembly of CQD Thin Films

As-synthesized CQDs are capped with long, organic ligands that passivate the CQD surface and allow their colloidal dispersion. These ligands also separate the particles when they are arranged one next to each other in a thin film, leading to insulating behavior; hence their removal or exchange is crucial in achieving electronic coupling between the CQDs. This exchange is typically done using layer-by-layer spin coating by alternating the deposition of the CQDs and the chemical treatment steps. Although the resulting films are smooth and macroscopically homogeneous, they lack the ease of processing, which is characteristic of other solution-processable semiconductors such as polymers. Moreover, the resulting films lack long-range structural order, a characteristic of inorganic semiconductors. To overcome the limitations of the layer-by-layer fabrication, two methods have been developed recently, tackling the ease of processing and the structural control.

2.1. Solution-Phase Ligand Exchange

The most established and successful method to fabricate CQD solids, namely, the ligand exchange performed on a solid film, results in cracked layers, often affected by incomplete reaction, and is highly time and resource consuming.[15,21] This practical bottleneck of forming high-quality, device-grade thick arrays in a single step limits the application prospects. In the last decade, a number of methods to perform ligand exchange in liquid phase prior to the formation of CQD solids were reported. The process is based on the replacement of the hydrophobic, organic ligands by small, highly charged inorganic species accompanied by the migration of the CQDs from the original apolar solvent to a polar one (**Figure 1**). The resulting, inorganic-capped CQDs form electronically coupled solids directly upon deposition, thus these versions of the CQD inks can be applied in any solution-based deposition techniques.

The chemical nature of the inorganic ligands varies a lot. The first reports on achieving colloidal stability in a fully inorganic compound semiconductor system introduces the use of chalcogenidometallate complexes (highly charged main group metal chalcogenide ions), and later simple chalcogenides, bichalcogenides, or thiocyanate.[22–26] The complex species used for stabilization usually take the $M(ox)_mE_n^{(2n-ox*m)}$ form, where 1–2 metal or semimetal cores (M^{ox+}: Sn(IV), Sb(V), Mo(VI), As(V), or Ge (IV), for example) are surrounded by a chalcogenide shell (E: S^{2-}, Se^{2-}, and Te^{2-}) and are countered by hydrazinium, ammonium, or alkaline metal ions in a highly polar media,

Daniel M. Balazs obtained a B.Sc. degree in chemical engineering in 2011 from the Budapest University of Technology, Hungary. In 2013, he gained his M.Sc. degree in the top master programme in nanoscience from the University of Groningen in The Netherlands. He specialized in the physics and chemistry of CQD assemblies in the Photophysics and Optoelectronics group of Prof. Maria Antonietta Loi at the Zernike Institute for Advanced Materials at the University of Groningen, where he obtained his Ph.D. degree in 2018. He is currently a postdoctoral fellow in the group of Prof. Tobias Hanrath at Cornell University, New York, USA.

Maria Antonietta Loi studied physics at the University of Cagliari in Italy, where she received her Ph.D. in 2001. In the same year, she joined the Linz Institute for Organic Solar Cells, University of Linz, Austria, as a postdoctoral fellow. Later, she worked as researcher at the Institute for Nanostructured Materials of the Italian National Research Council in Bologna, Italy. In 2006, she became Assistant Professor and Rosalind Franklin Fellow at the Zernike Institute for Advanced Materials of the University of Groningen, The Netherlands. Since 2014, she has been full professor in the same institution and chair of the Photophysics and OptoElectronics group.

such as hydrazine, formamide, or dimethyl-sulfoxide. Similarly, some metal chalcogenides (In_2Te_3, ZnTe, $CuInSe_2$, and Ga_2Se_3) in their molecular form stabilized in hydrazine also act as stabilizing ligands for various CQDs.[22] The process of the chalcogenide or chalcogenide-complex stabilization is driven by the high affinity of the chalcogenides to the reactive, unbalanced metal ions left at the surface after the removal of the original organic surfactants.[22]

Fully inorganic thin films can be formed by conventional techniques, such as spin coating, but the high boiling points of the solvents require higher processing temperatures, achieved by IR heating, for example.[27] Further annealing easily removes the volatile ammonium or hydrazinium cations, converting the ligand shell into an amorphous metal chalcogenide matrix. This approach enables the on-demand fabrication of nanostructured alloy materials based on high-quality, monodisperse CQDs, for example PbSe in Sb_2Se_3 or GeS_2, or PbS@CdS in As_2S_3.[23,28] The composition of the ligands can be matched to that of the

**ADVANCED
SCIENCE NEWS**

www.advancedsciencenews.com
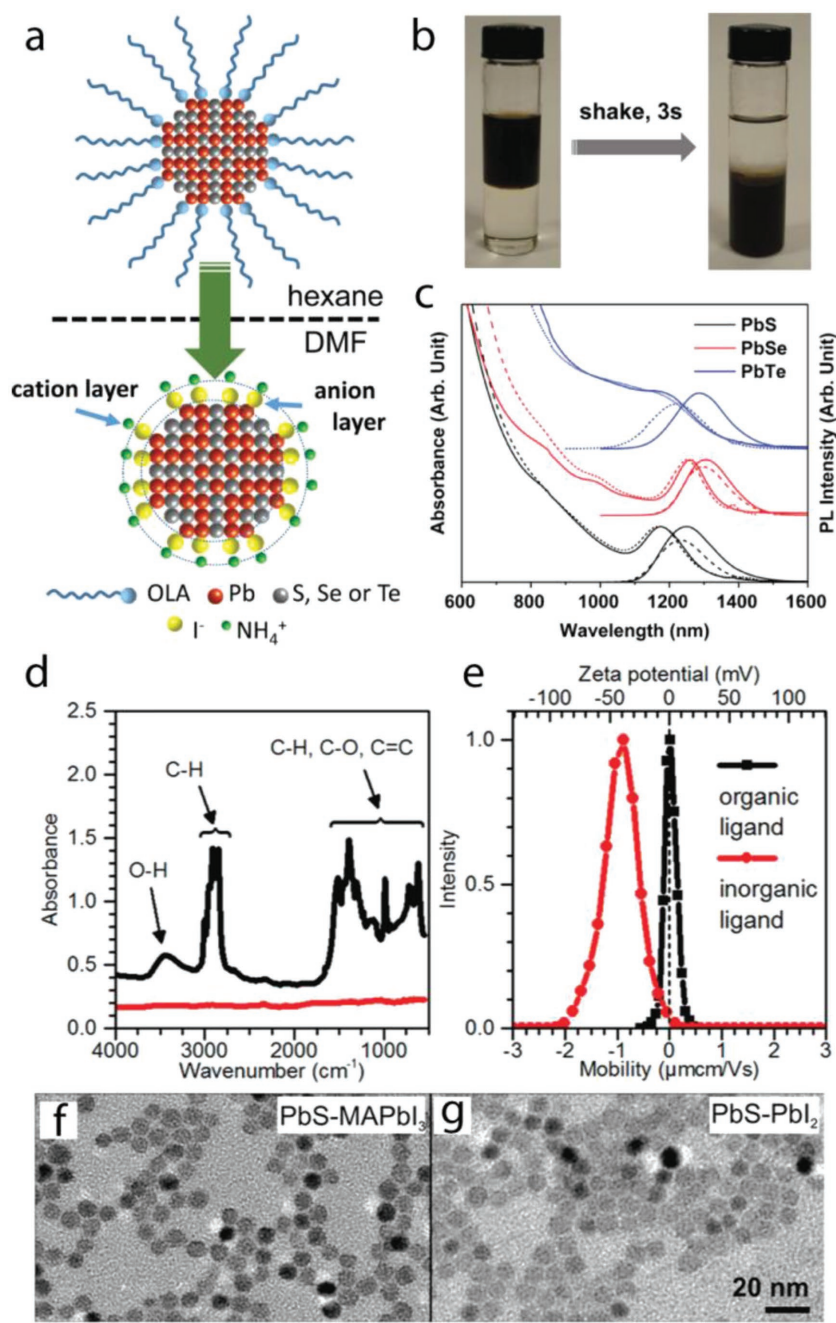
**ADVANCED
MATERIALS**

www.advmat.de

Figure 1. Phase-transfer ligand exchange: a) the CQDs are transferred from the original apolar phase to the polar one containing the new ligands while their ligand shell is replaced; b) the upper, apolar phase turns transparent, and the bottom, polar phase takes the color of the CQDs after successful ligand transfer; c) the absorbance and emission spectra before (dashed) and after (solid) the transfer show only minor differences, stemming from the changing dielectric environment; d) the lack of C–H, C–O, and C–C vibrations prove the replacement of the original ligands; e) the zeta potential of the CQDs indicates a heavily charged surface, suggesting the addition of excess ligands; f,g) the particle shape and size remain the same during the phase transfer, as seen under a TEM. a–c) Reproduced with permission.[45] Copyright 2017, American Chemical Society. d–g) Reproduced with permission.[37] Copyright 2017, American Chemical Society.

CQDs, creating a nanocrystalline, but chemically homogeneous material upon annealing.[29]

The chalcogenide-based stabilization showed very good prospects for charge transport in thin films,[10,18,24,30] but the

significant loss of quantum confinement and the low photoluminescence quantum yield after ligand exchange are disadvantageous for applications in solar cells or other optoelectronic devices.[28,31] Moreover, the need of the explosive hydrazine for the stabilization of the chalcogenide complexes and the lack of stability of the high-quality thiocyanate-capped CQD dispersions made the overall approach inconvenient.

Short molecules, similar to those used in the fabrication of the early CQD solar cells, allow for achieving charge transport while retaining the quantum confinement. For example, aryl- or alkyl-thiols have been shown to stabilize PbS CQDs in chlorinated organic solvents.[32–34] However, only partial investigations are available, and at this stage it is not possible to evaluate their performances in devices. Around the same time, the layer-by-layer ligand exchange using halides was introduced. The halides lead to great results in solar cell fabrication, showing not only increased performance, but also much better ambient stability than the organic ligands.[12,13,35,36] The realization of halide-capped solution-phase ligand exchange was therefore the next logical step in the process.

Following the metal-complex approach laid down earlier, a method of stabilizing CQDs in polar solvents using halides was developed. Species with the general structure of $M(ox)$ $X_n^{(ox-n)}$, where M is a metal cation with "ox" oxidation state and X is a halide, were shown to transfer various CQDs from an apolar to a polar phase by ligand exchange.[37] The formation of the stabilizing species occurs in dynamic equilibrium of the $[MX_{n-1}]^+$, MX_n, $[MX_{n+1}]^-$, $[MX_{n+2}]^{2-}$, etc., series. Self-ionization in a metal halide solution can readily result in sufficient conversion to ionic species, which can further be improved by adding alkaline or organic-ammonium halides. The phase transfer and ligand exchange occur using simple alkali- or (alkyl) ammonium-halide and pseudohalide solutions as well.[38,39] Moreover, the stabilization of halide-capped CQDs can be realized in purely ionic media; low melting point inorganic halide or nitrate mixtures and organic salts can form stable dispersions of various nanocrystals via phase transfer or dispersion of previously exchanged particles.[40]

The mixed solution of methylammonium-iodide and lead iodide is the simplest precursor for the formation of the MAPbI$_3$ perovskite semiconductor.[41] Epitaxial growth of a perovskite shell upon drying PbS dispersions stabilized by bismuth- or lead-iodide-based ligands has been reported.[42,43] These epitaxial shells provide

good surface passivation, as indicated by the PL quantum yield of MAPbI$_3$-capped PbS CQDs as high as that of the oleate-capped ones.[37] Moreover, the use of these ligands allows the easy fabrication of composites based on CQDs integrated into a perovskite semiconductor matrix.[44] Signatures of energy- and charge transfer between the CQDs and the matrix have been observed, showing the prospects of the method in forming heterojunctions at the nanoscale.[43,44]

Most inorganic-capped CQDs easily disperse in polar, high boiling point solvents, such as N-methylformamide (NMF), dimethylformamide, dimethylsulfoxide, or propylene carbonate. The stabilization occurs through dielectric screening of the ligand ion pairs: the halide anion acting similar to an X-type ligand remains bound to the CQD surface, while the cation is solvated. For this reason, donor-type solvents and additives (NMF or hexamethylphosphoramide) largely improve the stability of the dispersions.[37] The requirements of high polarity and simultaneous donor- and acceptor-type behavior keep the list of possible solvents short, and most candidates exhibit high boiling point. The most promising solvent reported for inorganic-capped CQD dispersions is 2,6-difluoropyridine, with a boiling point of 125 °C.[45]

The possibility of stabilization strongly depends on the CQD size. Lead-chalcogenide CQDs are faceted; in the few nanometer size range only a few facet types appear making them determinant for the overall properties. The whole surface consists of atoms with coordination number lower than the bulk value, but the actual coordination depends on the facet type. It has been demonstrated that the particle shape shows a transition from octahedron to truncated octahedron with increasing size at around 3–3.5 nm, causing the dominant facet to change from {111} to {100}.[46] The lower coordination of the {111} facets compared to the {100} ones leads to higher binding energy to the ligands.[47,48] Moreover, the {111} facets are typically lead terminated, while the {100} ones show balanced stoichiometry. These facts give rise to chemical differences of the facets, and in turn to size-dependent chemical properties of the CQDs. The most observable consequence of the size difference is the possibility to stabilize iodide-capped 2.9 nm PbS CQDs in n-butylamine, and the impossibility thereof using 4.6 nm particles.[49,50] Consequently, the ink formulation has to be adjusted to the particle size and shape.

2.2. Self-Assembly into Superlattices

The widely used layer-by-layer spin- or blade-coated films of CQDs are macroscopically homogeneous and smooth, but show clear nanoscale disorder both in the particle spacing and orientation.[15,21] The prospects of creating artificial, nanostructured assemblies of CQDs showing both crystal-like electronic and transport properties while maintaining the quantum confinement have encouraged researchers to find ways to controlling the assembly process. It has been known for 20 years that as-synthesized, organic-capped CQDs tend to form ordered structure upon controlled precipitation from solution.[51] The supercrystal symmetry and the orientation of the individual CQDs within the lattice are strongly affected by the particle shape and ligand coverage.[52,53] Mild annealing of these

supercrystals leads to the formation of narrow interparticle connections, named "necks."[54] However, from a practical perspective, arrays where the original ligands are fully and controllably replaced are of greater scientific relevance.

Oriented attachment of lead-chalcogenide CQD thin films can be achieved through desorption of the ligands induced by chemical treatment of a solid film.[55,56] The chemical treatment can be simply the exposure to a liquid that dissolves oleic acid (L-type ligand replacement in Green's formalism) or lead oleate (removal of a Z-type ligand), or to a solution containing reactive species that replace the oleate groups (X-type ligand replacement).[21,55–59] However, the formed layers are not continuous due to the shrinkage occurring during the ligand replacement, and only short-range ordering is observed in lack of full rotational freedom.

Long-range order can be achieved by forming thin films on top of a liquid bath, where CQDs maintain their rotational and translational freedom during the assembly process (see the schematic in **Figure 2**).[60] The self-assembled structures can be irreversibly stabilized by inducing an oriented attachment; the ligand desorption in this case can be triggered by heating a mildly reactive subphase liquid or injecting chemical agents into the bath.[61–65] Optimizing the method, superlattice domains of several micrometers can be achieved, and the properties of the structures can be studied. The interest in these structures has recently been validated by two works reporting record charge carrier mobilities in PbSe CQD superlattices, with a clear improvement compared to what is found in traditional disordered arrays.[66,67]

The superlattice formation mechanism is influenced by the faceted nature of lead-chalcogenide CQDs. By default, isotropic, quasispherical particles with rather dense and hard ligand shells assemble into face-centered cubic (FCC) superlattices with random orientation of the single particles. Typical lead-chalcogenide CQDs are faceted, with octahedral (for smaller particles) or truncated octahedral/rhombicuboctahedral (for larger diameters) shape.[46] The shape anisotropy itself can lead to different superlattice symmetry with a preferred orientation due to shape-exclusion effects (increased packing density) and orientation-specific interactions.[53,69] These interactions are more pronounced in the case of a thinner, anisotropic, or missing ligand shell, which is achieved upon chemically or thermally triggered ligand exchange or removal. The different coordination numbers at the main facets resulting in different ligand binding energies make the ligand desorption easier from the {100} facets.[47,56] The consequent appearance of large, uncovered surface areas at given directions, with highly enhanced orientation-specific interactions and capacity to fuse, drives the formation of close-to-square, rhombic ordering in monolayers, and body-centered cubic (BCC), rhombohedral, or (almost) simple cubic order in multilayer samples, with the {100} facets facing the subphase.[67,68,70,71] The uncovered, reactive facets tend to epitaxially fuse through surface diffusion of atoms into the gap, resulting in a semiconnected structure, where some connections (necks) are as wide as the interacting facets, but the rest of the necks are missing and the gap increased.[67,72]

In practice, CQD superlattices go through most mentioned phases during the superlattice formation (see Figure 2b).[70] Before the solvent dries, no disorder is observed.[73] As the CQD

ADVANCED
SCIENCE NEWS

www.advancedsciencenews.com
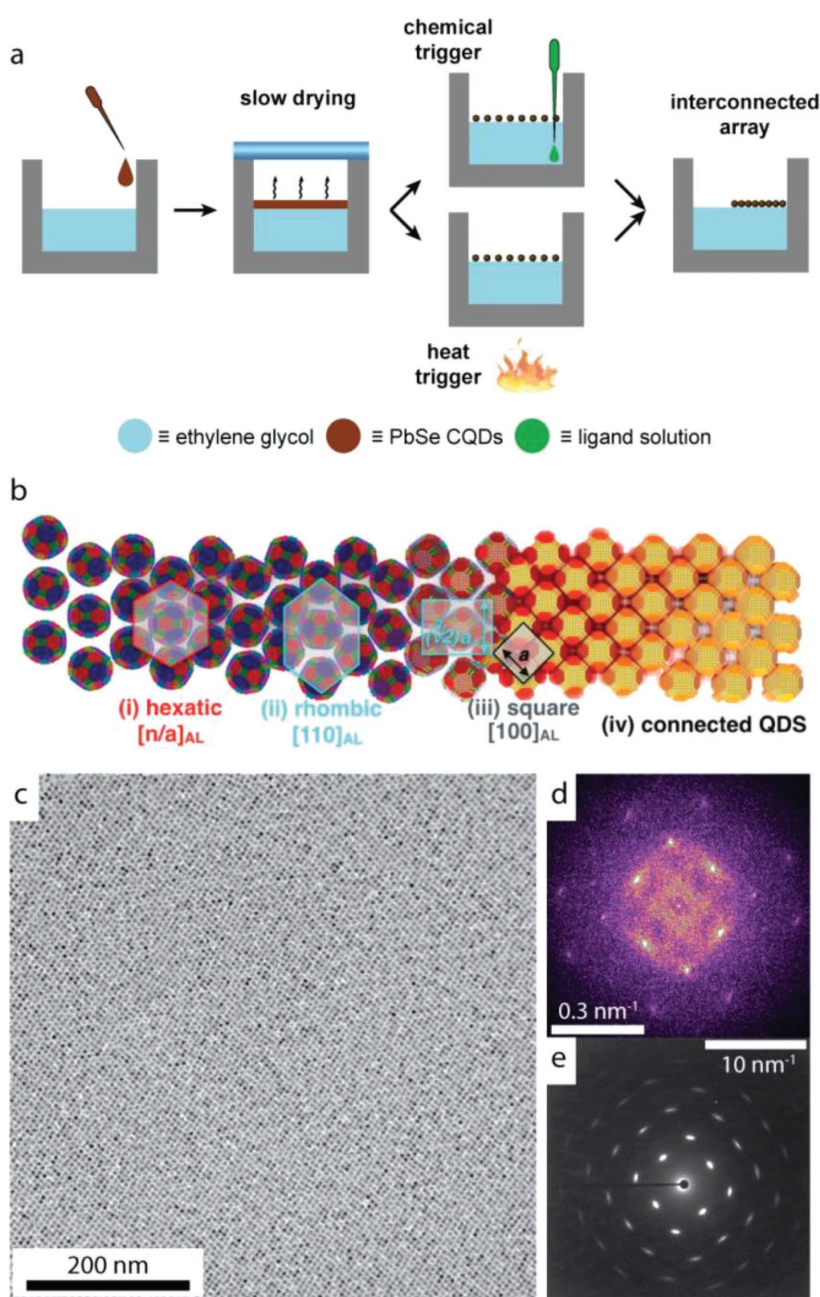
ADVANCED
MATERIALS

www.advmat.de

Figure 2. a) Schematic of the liquid-supported superlattice growth process: the CQD solution is dropped on top of a liquid surface, the solvent is slowly evaporated, and the ligand desorption is triggered chemically or by heat; b) the CQD array goes through several structural phases upon superlattice formation, starting from a disordered, glassy phase through FCC and BCC structures to cubic symmetry; c) long-range ordering in a close-to-square PbSe superlattice; d) superlattice order visualized applying fast-Fourier transformation on a large-area TEM image (data from panel (c)); e) the orientation of the CQD atomic lattices can be tested by selected-area electron diffraction (the image shows a PbSe CQD lattice from the (100) zone axis). a,c–e) Reproduced with permission.[67] Copyright 2018, The Author. b) Reproduced with permission.[68] Copyright 2017, American Chemical Society.

concentration increases, a hexagonal/FCC layer forms since the ligand shell is swollen by the solvent. Upon drying, the hexagonal structure turns into a BCC one. The final stage of the transformation takes place upon chemical or heat trigger.[64,67,68]

By limiting the ligand desorption to the {100} facets and keeping the original FCC-type lattice, a honeycomb structure can be formed, where instead of the ligand-free {100} facets, the ligand-covered {111} ones are parallel to the substrate, and two hexagonal layers of CQDs are interconnected by out-of plane bonds. Simultaneous optimization of the reactivity of the subphase for ligand desorption, the miscibility of the ligand shell, and the subphase to orient the CQDs and the CQD concentration is necessary to achieve this structure.[61] Such an optimization is highly complex, and the fabrication of honeycomb superlattices has only been reported once using ethylene-glycol subphase, oleate-capped PbSe CQDs, and heating to desorb the ligands.[74]

2.3. Disorder in CQD Solids and the Possibility of Band Transport

The interest in ordered CQD arrays stems from the prospect of achieving coherent transport through extended states, similar to the behavior observed in macroscopic crystals. This phenomenon is expected to be controllable by the structure of the layer, leading to materials with tunable confinement and dimensionality with more flexibility than in bulk crystals. The desire to deliver proof for coherent transport led to reports on partial or inconclusive experimental results accompanied by strong statements, and followed by criticisms of the criteria used to prove transport through extended states.[75,76] In this section, we give a brief introduction to the topic and a critical overview about the state of the art at this stage.

Objects with discrete energy levels, when in proximity, show electronic coupling and extension of the electronic states; the strength of this effect is dependent on the distance and the barrier height. Moreover, in the presence of translational symmetry (e.g., in a superlattice of nearly identical CQDs), the coupled states can extend to long range. An array of ideal interacting particles can show different "phases" based on the relation of the charging energy (E_C) and the coupling strength (β). At sufficiently large E_C, the charge carrier localizes on one site (Mott insulator), while a high coupling energy leads to complete delocalization. This metal–insulator transition has been experimentally shown in a monolayer of silver nanoparticles controlled in a Langmuir trough.[77]

If the two objects (and therefore the energy of the two interacting states) are slightly different, the energy mismatch also

plays a role in determining the coupling strength. In a non-ideal array, the presence of energetic disorder brings in another phase, the domain localization. In these systems, the carriers are delocalized over a number of sites (particles), surrounded by a shared, higher barrier.

In realistic CQD arrays, significant disorder is present. The main source is the variation in the confinement energy due to slightly different sizes. Current synthesis techniques are capable of producing CQD batches with diameter variation below one atomic layer, $\partial d/d \approx 3\%$ precision.[78] Such CQD dimension variation leads to an approximate energy disorder of $\partial E/E \approx 2.5\%$, a value in the tens of meV scale in highly confined, 3–4 nm diameter PbS CQDs.[75,79,80] Further sources of the energetic disorder are inhomogeneous coupling due to positional disorder and charging energy disorder due to inhomogeneous assembly or surface termination (permittivity), or trapped charges (local electric field). In lead-chalcogenide CQDs, however, the charging energy is usually similar or lower than that stemming from the disorder, setting the latter as the dominant factor.[75]

On a macroscopic scale, a multitude of interacting quantum dots is expected to form bands with bandwidth being dependent on the coupling strength. The energetic disorder also results in a quasicontinuous, Gaussian-like distribution of states with a characteristic width. Pure band transport can only be observed in systems with coupling bandwidth larger than the width of the state energy disorder. Consequently, reports claiming band-like transport should include detailed estimation of the energetics of the system.

Currently, the typical figures of merits used to determine whether the carriers are transported through extended state and not through a series of hopping events are i) negative dependence of the mobility on the temperature; ii) mobility values above 1 cm² V⁻¹ s⁻¹; and iii) the observation of Hall effect in the sample. In practice, these conditions have often been used arbitrarily, separately, and without proper interpretation. Recent works of Guyot-Sionnest and Scheele have given a detailed overview of the possible flaws in the evaluation of these criteria; here we summarize the most important aspects.[75,76] Briefly, neither of the aforementioned criteria can be considered individually as direct proof for band transport, but a combination of the different results is necessary.

i) A "false positive" observation of negative dependence of the mobility on the temperature (assumedly the signature of phonon scattering–limited transport) can be explained within the framework of thermally assisted hopping using the classical Marcus's theory of activation.[81,82] In this approach, the hopping event takes place if the reorganization energy is higher than the electronic coupling, and calculations show that in realistic samples, phonon-assisted hopping is the charge transfer mechanism.[81,83] Although it has not been proven experimentally, a system can reach the "inversion" region at temperatures higher than E_a/k_B, where E_a is the activation energy of the given process, resulting in a decreasing reaction rate with temperature.[84] This principle applies for hopping transport in disordered materials, requiring careful evaluation of the low-temperature activation energy and temperature range where the negative temperature coefficient is

observed.[75] A similar relationship can be obtained based on the Einstein relation for transport as a series of single hopping events.[75]

ii) The criterion of mobility values >1 cm² V⁻¹ s⁻¹ suggesting band transport was originally suggested for small molecule single crystals based on the lattice periodicity. However, due to the one magnitude higher structural features (CQD diameter or spacing), the expected value should be set to >10 cm² V⁻¹ s⁻¹ for CQD solids. Such values are rare, but possible to achieve in sintered CQD solids. However, values in this order of magnitude are theoretically predicted for charge carrier or polaron hopping as well, and thus the criterion is of low reliability.[75,83]

iii) Hall effect has been observed in disordered systems, but the Hall-mobility values are often far from those obtained from other methods.[85,86] However, due to the possible coexistence of variable range hopping and reasonable Hall mobility,[87] and the possibility of Hall effect in polaronic systems,[88] this criterion can only indicate good conductivity and not band transport.

However, if multiple criteria are considered, one can rule out hopping-like processes. Negative temperature coefficient at temperatures below E_a/k_B and the presence of Hall effect with Hall mobility in the same order of magnitude as the field-effect mobility in the same temperature range, with values well above 10 cm² V⁻¹ s⁻¹, can indicate band transport. Moreover, the analysis should include an appropriate estimation of the disorder and the average coupling strength in the system.[76] A good example for such a detailed study is the work of Whitham et al., where they estimate the carrier delocalization based on low temperature mobility data, structural studies, and electronic structure calculation based on the experimental data.[89] Recently, electron mobilities approaching the values measured in champion, sintered CdSe CQD films have been measured in highly ordered, epitaxially connected, but confined PbSe CQD superlattices, which are likely next to be tested for the transport mechanism.[66,67]

3. Surface-Based Control of the Electronic Properties

The interest toward CQDs stems, besides from the fascinating, tunable optical properties, from the promise of excellent tunability of the electronic properties. For example, the formation of junctions in bulk materials can only be achieved by ion bombardment doping or interfacing different materials. On the other hand, the large surface area of CQD solids gives researchers a tool to control the properties during synthesis or deposition at the nanoscale, yet having a bulk effect. This aspect is especially relevant for the facile fabrication of (opto)electronic devices. In the following, we discuss the recent developments in the electronic property control that shows the true value of CQD solids.

During the first few years of investigations, CQD solids were mainly treated with thiols for enhanced coupling and conductivity, reaching mobilities in the range of 10^{-3}–10^{-2} cm² V⁻¹ s⁻¹ with a very limited on/off ratio.[3,6] From that point on, the control of the polarity or charge carrier density has been the focus of researchers as the bottleneck in materials development.

**ADVANCED
SCIENCE NEWS**

www.advancedsciencenews.com

**ADVANCED
MATERIALS**

www.advmat.de

Figure 3. Methods to control the polarity in CQD assemblies: a) the surface ligands modify the CQD internal electric field through their dipole moment; b) charge-transfer molecules with high ionization potential or electron affinity cause moderate Fermi-level shifts and more significant changes in the band edge positions; c) stoichiometric adjustments leading to polarity changes in CQD solids. a) Reproduced with permission.[102] Copyright 2014, American Chemical Society. b) Adapted with permission.[105] Copyright 2016, American Chemical Society. c) Upper panel: Adapted with permission.[55] Copyright 2014, American Chemical Society. Lower panel: Adapted with permission.[114] Copyright 2017, The Authors, published by American Association for the Advancement of Science.

These films were highly sensitive to air and water in the fabrication and measurement environment, which resulted in predominant p-type doping.[90] Proper control of the fabrication environment led to the realization that thiol-capped CQDs can also show excellent, electron-dominated ambipolar properties, but the air sensitivity remained a problem.[91]

The introduction of atomic, halide capping for PbS CQDs gave a partial solution. Replacement of the original oleate shell with a halide (mainly iodide) atomic layer results in high mobility and air-stable n-type thin films.[13] The method resulted to be robust, and the halides were used with various (alkaline, ammonium, and organic ammonium) counterions dissolved in polar solvents.[11] The only requirement is the solubility of the oleic acid in the solvent and the presence of acidic species to catalyze the ligand exchange.[21,56,92,93]

With the realization of air-stable samples and the growing, solid knowledge on the CQD chemistry, researchers turned toward controlling the electronic properties for applications.[94]

In bulk materials, vacancy creation or heteroatom substitution can lead to dominance of one carrier type due to the locally different number of electrons. Accordingly, plasma-synthesized silicon nanocrystals can be doped with the traditional, boron- or phosphor-incorporation method.[95] In solution-prepared nanomaterials, however, this approach is less effective due to the synthesis process; many materials form highly perfect nanocrystals due to facile rearrangement, "self-purification," during the crystal growth.[96] This refinement leads to segregation of the dopants at the CQD surface limiting the effectiveness of the method.[97,98]

Alternatively, several novel methods have been developed to control the polarity or charge carrier concentration in CQD solids (see **Figure 3**); most of them exploit the uniquely large surface area of the particles. Attachment of ligands carrying dipoles to the CQD surface has been shown to modify the CQD's internal electric field, similar to self-assembled monolayers affecting the work-function of metal surfaces

**ADVANCED
SCIENCE NEWS**

www.advancedsciencenews.com

**ADVANCED
MATERIALS**

www.advmat.de

(Figure 3a).[99–101] The effect has been observed using the thiol and the halide ligands as well. The energy level differences are sufficient to form quasi-pn junctions using a bilayer of the same CQDs with different ligands, opening ways for applications.[102] However, the achieved level of doping is insufficient for optimal application in electronic or thermoelectric devices.

Recently, the carrier concentration has been adjusted by inserting organic or metal–organic molecules with high ionization energy or electron affinity into the CQD films (see Figure 3b).[103–107] The charge transfer process between the molecules and the CQDs results in localization of one carrier, creating a population of free, unbalanced carriers of the other sign, similar to a classical doping effect. Moreover, organic molecules (both ligands and additives) in CQD films can affect the electronic coupling between the adjacent dots. Tuning the (mis)alignment of the HOMO or LUMO of the molecule with the matching states in the CQDs allows for suppressing or enhancing the coupling for one of the carriers, and determining changes in the apparent device polarity.[104,108] Addition of ligands can also modify the density of states of the single CQDs, as observed from the increased absorbance of CQDs capped with arene-thiolates, and the effect can be fine-tuned with functional side groups attached to the aromatic ring.[109–113]

In contrast to the limitations set by the "self-purification," the small size can also enable the introduction of more vacancies in weaker crystals through stronger strain relaxation. The few working examples of such doping are all observed in copper-based chalcogenides ($Cu_{2-x}S$, $Cu_{2-x}Se$, and $Cu(In,Ga)Se_2$), where copper vacancies are frequently present, giving rise to hole doping.[115,116] The overall effect of the stoichiometric imbalance strongly depends on the nature of the vacancies/excess atoms. In bulk state of polar semiconductors, the charge neutrality requirement leads to excess holes or electrons for every vacancy/excess atom. Similarly, the addition of neutral metal or chalcogene to a CQD array (e.g. through thermal evaporation) leads to a strong doping (Figure 3c).[117,118] In nanomaterials, on the other hand, stoichiometric imbalance of charged species can easily be shielded by counterions at the surface. However, due to the small size, a few excess atoms of either component lead to a large off-stoichiometry.[119] In this case, only the band structure is expected to change—increasing density of states in the valence or conduction band with the excess of the anion or cation—leaving the overall carrier concentration unaltered.[114] Experiments in lead- and cadmium chalcogenides have shown an effective p-type doping as a response to treatment with chalcogenide salts that may stem from a not only changed, but also shifted energy levels, likely through surface dipoles or partially oxidized chalcogenide ions.[55,114,120,121] On the other hand, the addition of lead- or cadmium salts results in partial restoration of the original behavior.

4. Prospects in Energy Harvesting and Optoelectronics

4.1. Solar Cells

The realization of stable n-type lead-chalcogenide CQD solids gave a boost to the development of CQD solar cells. Previously,

the air-sensitive and consequently mostly p-type thiol-treated arrays were used in Schottky-type or in the so-called depleted heterojunction solar cells.[122,123] Using a thick halide treated n-type layer and a thin thiol-treated layer on top, the currently best device structure was developed, where the charge carrier extraction is facilitated (**Figure 4**a–c).[35] In these devices, the ligand-dependent position of the energy levels in the two layers is exploited, forming a quasi-pn type-II heterojunction.

Almost at the same time, the solution-phase ligand exchange was introduced to the solar cell research as well.[49,124] While by using thiol-only stabilization the device performances are as low as the layer-by-layer-treated thiol-based samples,[32,33] the possibility of mixing CQDs stabilized with different ligands enables the formation of a bulk heterojunction–like device architecture that carries the possibility of fine-tuning the carrier extraction to the electron and hole mobilities in the material.[125] The use of stable dispersions of ligand-exchanged CQDs allowed for the fabrication of polymer:CQD bulk heterojunction solar cells with decent efficiencies.[111] Refinement of the ligand exchange chemistry for lower trap density and disorder recently led to an improvement in the efficiencies, up to a record of 11.3%.[19,126] Although the lower energetic disorder results in increased open-circuit voltages in these solar cells (see Figure 4d–f), the values are still not competing with those of other solution-processable semiconductors as the hybrid perovskites. The suppression of the density of carrier traps and recombination centers is crucial in improving the solar cell performances.

The superior quality of the halide-capped materials, their n-type character, and the dominance of the electron transport due to the stoichiometric imbalance led to a bottleneck in the further improving this device performance. A low depletion width in the thick n-type layer caused by a low hole concentration in the p-type one was found to be the limiting factor in the current device structure.[128] Since the n-type material is generally of higher quality in terms of trap concentration and air stability, methods of achieving a higher hole concentration in the p-type layer were proposed to solve the bottleneck (Figure 4g,h). The treatment with a chalcogenide solution, which modifies the band structure and results in an effectively more p-type material, and the doping with charge-transfer molecules lead to an increased hole concentration.[107,127] Although these methods tackle the problem, the hole mobility in the highest quality CQD films is still orders of magnitude lower than the electron one. Wider applications require both efficient electron and hole transport, setting the direction of the research for the next few years.

4.2. Electronic Devices: Field-Effect Transistors (FETs) and Inverters

Field-effect transistors, besides being the fundamental building blocks of modern electronics, are often used to characterize the transport properties of semiconductors. For this purpose, mainly simple device structures (bottom-gate, bottom-contact, and Si/SiO_2 wafer as the gate stack) are used, optimized for parameter screening and convenient lab-scale fabrication. However, many improvements have been made to the material
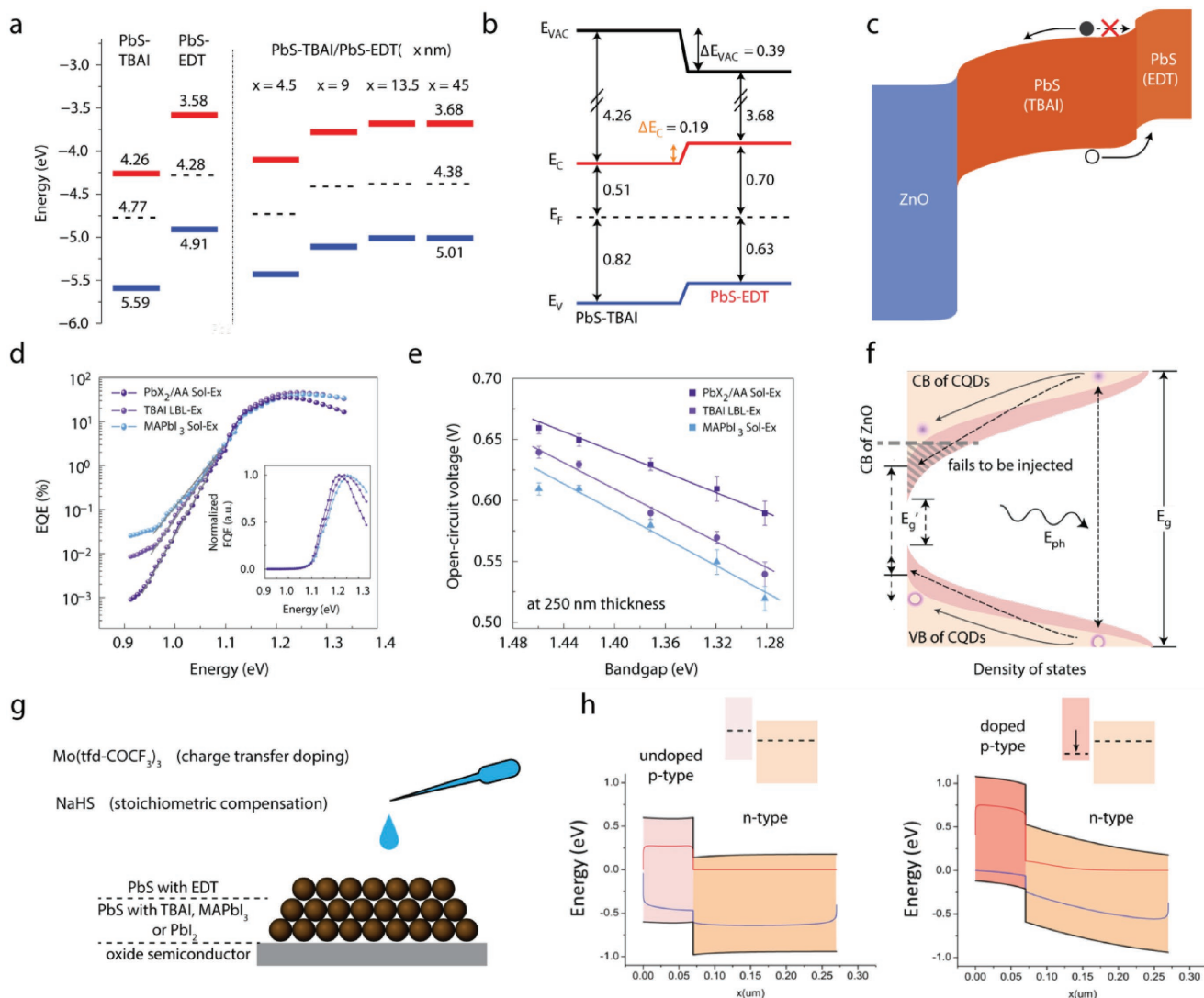
**ADVANCED
SCIENCE NEWS**

www.advancedsciencenews.com

**ADVANCED
MATERIALS**

www.advmat.de

Figure 4. Developments in the CQD solar cell structure and proposed solution for the hole bottleneck: a) ligand-dependent band edge positions in PbS CQD solids lead a depletion region in bilayer structures; b,c) the bilayers form a quasi-pn junction that enables the fabrication of efficient solar cells using only an electron-selective electrode; d–f) refined ligand exchange recipe resulting in lower polydispersity and energetic disorder in the deposited thin films resulting in: d) a sharper absorption edge and e) higher open-circuit voltage measured in solar cells; f) electron injection into the electrode is improved in less disordered samples due to the shallower band tail; g) hole doping of the p-type layer with a metal-organic molecule and stoichiometric adjustment were suggested as methods to improve the performance;[107,127] h) doping the EDT-capped layer increases the depletion width in the n-type absorber, improving the carrier extraction. a–c) Reproduced with permission.[35] Copyright 2014, Springer Nature. d–f) Adapted with permission.[19] Copyright 2016, Springer Nature. h) Adapted with permission.[107] Copyright 2017, American Chemical Society.

chemistry and the device structure to boost their performance for practical purposes, and several attempts were aimed to create more complex electronic circuits (see an overview in **Figure 5**). The main interest in CQD FETs lies in the tunable electronic properties: the possibility of fine-tuning the carrier concentration and mobility in a simple manner carries enormous prospects for applications.

The first high-mobility CQD FETs were fabricated based on chalcogenidometallate- or thiocyanate-stabilized inks (more information about the chemistry was discussed in Section 2.1).[24,30,129,130] This approach resulted in good transport with an electron mobility of 10–20 cm^2 V^{-1} s^{-1} in CdSe CQD arrays. However, this approach should mainly be

considered as an alternative fabrication method for thin film compound semiconductors, as the confinement is mostly lost in the annealing process). The first FETs based completely on nanocrystal inks were reported recently as to show the prospects of this fabrication approach (Figure 5a–c).[131] In this work, the CdSe CQD channel is controlled by a colloidal Ag/colloidal Al$_2$O$_3$ gate stack and contacted by electrodes based on a mix of In and Ag nanoparticles. Between the deposition steps, each layer is always functionalized by a ligand treatment to protect the film and to enhance the wetting for next layer.

Keeping the focus on the bottom-up fabrication of thin film compound semiconductors, the method has been refined to match the composition of the stabilizing and connecting
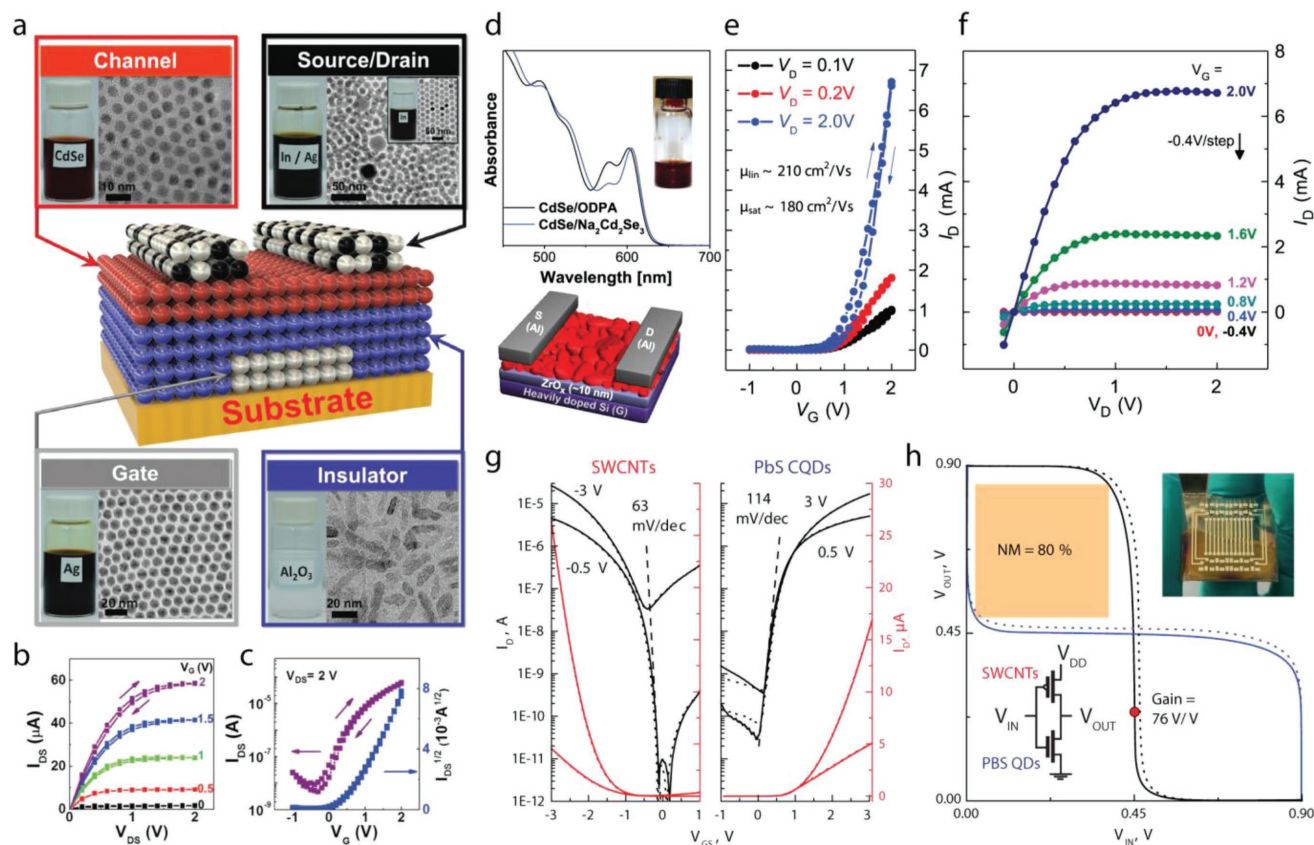
Figure 5. Recent developments in CQD FETs and logic circuits: a) fully colloidal-nanocrystal-based FET using CdSe CQDs as the channel material, Al_2O_3 as the gate dielectric, and a mix of In and Ag nanocrystals as the contacts; b,c) output and transfer characteristics of the fully nanocrystal-based FET; d) absorbance of CdSe CQDs stabilized by a composition-matched $Na_2Cd_2Se_3$ ligands and the structure of the optimized FET; e,f) transfer and output characteristic of an FET showing behavior approaching that of the polycrystalline thin films; g) transfer characteristics of the optimized p-type carbon nanotube and n-type PbS CQD FETs; and h) a CMOS-like inverter based on these two units. a–c) Reproduced with permission.[131] Copyright 2016, American Association for the Advancement of Science. d–f) Reproduced with permission.[29] Copyright 2015, American Association for the Advancement of Science. g,h) Adapted with permission.[20] Copyright 2017, The Authors, published by Wiley-VCH.

ligands and the CQDs resulting in electron mobilities of several hundred $cm^2 V^{-1} s^{-1}$, approaching that of the polycrystalline bulk materials (Figure 5d–f).[18]

However, the loss of confinement is detrimental for light-related applications, such as light-emitting field-effect transistors or phototransistors. The confinement can be retained by using halides as capping or stabilizing ligands.[21] Layer-by-layer processed PbS or PbSe CQD FETs with iodide treatment were shown to give mobilities in the range of 0.1 $cm^2 V^{-1} s^{-1}$ and high on/off ratios.[13,55,106] Solution-phase treated, single-step deposited samples of halide-capped CQDs are sparse, but report very similar properties, opening the way for further, more application-oriented developments.[132,133]

The ligand-exchanged inks have another advantage besides the facile device fabrication, namely, the possibility of doping without an extra step in the process. Tuning the stoichiometry with the ligands or charge transfer molecules as described in the previous step requires an extra fabrication step, often for every deposited CQD layer.[106,114] This step can be avoided by mixing the dopant in the ink, making the films processing easier.[45]

The fabrication of high performing and stable FETs motivated researchers to test the materials in more complex devices. Inverters are the simplest examples: they consist of two, connected transistors. In the first attempt, complementary metal–oxide–semiconductor (CMOS)-like inverters were made using highly ambipolar, thiocyanate-capped PbS CQDs.[10,134] In these devices, because of the lack of complementary behavior, the leakage through the "off" device limits the performance. More advanced devices such as NMOS inverters, amplifiers, or ring oscillators on flexible substrates have been prepared using thiocyanate- or chalcogenidometallate-capped, sintered CdSe CQDs.[135,136]

The halide-capped, n-type CQD solids often outperform the chalcogenide-capped ones in subthreshold swing and on/off ratio, making their use preferred as the n-type component in electronic devices.[21] This is especially true, when the polarity of the FETs is fine-tuned with the choice of ligand and the electrode material.[137] The lack of high-quality p-type CQD FETs with similar sharp switching is the current limiting factor in the development of all-CQD electronics. However, combining the CQDs with another promising class of solution-processed semiconductors has been suggested recently (Figure 5g,h).

Semiconducting carbon nanotubes wrapped with a polythiophene derivative are known to form high-performance p-type FETs[138] and are excellent complementary material for iodide-treated PbS CQD solids. The combination of these two materials as elements of CMOS-like structures led to the best fully solution-processed inverters to date.[20]

Exploiting the quantum-confined and ambipolar nature of the CQDs, light-emitting FETs can be fabricated.[139] In these devices, the presence of both carriers controlled by the gate and the drain bias leads to localized recombination in the channel. The spectrum of the emitted light can be fine-tuned by the bandgap of the channel material, and therefore, the size of the CQDs.

The quantum-confined electronic structure of the CQDs can further be exploited in ionic-liquid-gated FETs.[140] In these devices, the charge carrier density in the channel is controlled by the potential of a liquid electrolyte. The extreme effective capacitance of the liquid dielectrics allows for determination of the bandgap and the spacing of the energy levels, and modulation of the charge carrier mobility and optical properties by controlling the band filling.[141–144] The high induced carrier density is also helpful in passivating trap states and characterization of heavily doped, or strongly coupled, low-bandgap CQD arrays.[8,15,67,97,114]

As an interesting outlook, colloidal tetrapod nanocrystals have also been tested and shown to be excellent candidates for flexible devices.[145] FETs formed with a random tetrapod network in the channel show a strong dependence on the length of the tetrapod's arm, indicating that the number of connection points increase with the arm length. The increased network connection density leads to better resistance against bending in the sense that the long arm tetrapods show much large conductivities at the same bending radius than the short arm ones. Also in flexible devices, both the electron mobility and the threshold voltage exhibit a bending radius dependence and hysteresis upon a complete bending cycle in PbS CQD FETs, suggesting reversibly changing ligand connectivity.[146]

4.3. Thermoelectric Energy Harvesting

The interest in nanostructured thermoelectric materials stems from the suppressed phonon mean path due to scattering at grain boundaries and the corresponding low thermal conductivity. In general, the higher the thermal gradient the higher the maximum power extractable from the device. Following this logic, most researchers focus on forming bulk thermoelectric materials with nanoscale structural features (domains, inclusions, superlattice periodicity, etc.).[147,148]

In an ideal thermoelectric material, the Seebeck coefficient, and the electrical and the thermal conductivity are separately optimized for maximum efficiency. CQDs are ideal building blocks for nanostructured thermoelectric materials for their diameter defining the feature size, the broad variety of available materials (allowing for alloying and compound formation), and all the methods developed to tune the electrical properties and optimizing the carrier concentration.[5] The surface-based approaches developed for CQD devices work for hot-pressed, sintered samples as well; n-type materials can be formed using halide treatment on lead-chalcogenide

CQDs before sintering, while stoichiometric (over)compensation of similar particles by alkali chalcogenides leads to p-type solids.[149,150] Engineering the potential landscape in bottom-up fabricated solids is possible through inclusion of metal nanoparticles, enhancing the thermoelectric response, while alloying is possible through mixing different CQDs (e.g., PbS and PbTe).[151,152]

Confined CQD solids are even more interesting for thermoelectric applications for the expected enhancement in the Seebeck coefficient due to the low dimensionality.[153–155] Quantum wells, nanowires, and 2D electron gases have shown increased thermal voltage that can be explained by their unique band structure.[148] Similar behavior enhanced by a possible band formation (only a narrowed density of states being available for transport) is expected for CQD assemblies.[156] Besides the interesting electronic structure, organic-capped, fully confined CQD arrays exhibit an order of magnitude lower thermal conductivities than the hot-pressed, sintered CQD-based materials. Moreover, it only increases by a factor of 2–3 (giving similar results to what has been observed in semiconducting polymers) upon exchanging the ligands without sintering, pointing toward prospective improve thermoelectric efficiencies.[157]

Enhanced Seebeck effect and over 1 mV K^{-1} Seebeck coefficient has been reported in PbSe and PbTe CQD arrays treated with hydrazine.[158,159] The doping effect of hydrazine was shown through the changing sign of the thermal voltage upon evaporation of the molecules. The Seebeck coefficient was found to be dependent on the particle size due to the changing energy level spacing in the array, a clear sign of a confinement-related behavior. Flexible thermoelectric devices based on p- and n-type CQDs have been reported showing good performances for a series of p–n units.[160] Despite the large thermoelectric effect, the power conversion efficiencies are limited due to the low conductivities; therefore a strong increase in the mobility is required to exploit the enhanced thermoelectric effect with the optimal carrier density.[158]

Thermal energy harvesting is not only possible through the Seebeck effect, but also absorption of IR photons can lead to energy conversion. In the previously described pn-junction structure (Section 4.1), low-bandgap CQDs show significant photocurrent when illuminated with a blackbody emitter.[161]

5. Conclusion and Outlook

CQD solids have great prospects in at least three main directions: i) the superlattices of CQDs with partial bulk crystal-like behavior and tunable dimensionality carry the promise of exploiting many confinement-based phenomena; ii) used as quantum-confined systems for light-coupled devices (solar cells and light-emitting field effect transistors), higher efficiencies and more flexibility in the device design are expected, showing commercial prospects; iii) as building blocks for bottom-up fabricated bulk materials for thermoelectrics, they show adjustability of the nanostructure and properties, with the added value of the ease of processing. While the prospects are visible, the progress is slower due to the need for deeper knowledge in the freshly developed synthetic, deposition processes and in the tuning of the electronic properties.

As discussed in Section 4, devices based on CQD solids start to reach levels of significant practical interest. Based on the solution-phase ligand exchange, bottom-up synthesis of bulk materials is already feasible for thermoelectric, electronic, and solar energy harvesting applications. Further improvements in the property control and ease of fabrication will further increase the interest, likely leading to commercialization.

The main directions to be researched in the coming years are fairly clear. For large-scale fabrication, the most important task is to expand the list of possible solvents with processing-friendly, low-boiling point candidates by improving the stabilization. The formation of high-quality p-type layers with improved hole mobility and resistance to sintering as in the halide-capped layers is the next step in property control, being relevant for all three main directions (solar cells, electronics, and thermoelectrics). For practical applications, more attention has to be given to devices fabricated by upscalable methods, even by compromising eventually on the device performances. At last, for environmental reasons and social acceptance Cd compounds should be avoided, together with harmful solvents, while Pb chalcogenides can be used for applications in energy harvesting in agreement with the most severe environmental legislations.

Finally, CQD solids appear to be not only an excellent "playground" for researchers from different disciplines (e.g. chemists, material scientists, condensed matter physicists), but also have serious chances to be utilized soon in electronic and optoelectronic devices.

Conflict of Interest

The authors declare no conflict of interest.

[1] A. J. Nozik, M. C. Beard, J. M. Luther, M. Law, R. J. Ellingson, J. C. Johnson, *Chem. Rev.* **2010**, *110*, 6873.

[2] J. Y. Kim, O. Voznyy, D. Zhitomirsky, E. H. Sargent, *Adv. Mater.* **2013**, *25*, 4986.

[3] F. Hetsch, N. Zhao, S. V. Kershaw, A. L. Rogach, *Mater. Today* **2013**, *16*, 312.

[4] S. Z. Bisri, C. Piliego, J. Gao, M. A. Loi, *Adv. Mater.* **2014**, *26*, 1176.

[5] S. Ortega, M. Ibáñez, Y. Liu, Y. Zhang, M. V. Kovalenko, D. Cadavid, A. Cabot, *Chem. Soc. Rev.* **2017**, *46*, 3510.

[6] D. V. Talapin, J. Lee, M. V. Kovalenko, E. V. Shevchenko, *Chem. Rev.* **2010**, *110*, 389.

[7] M. Law, J. M. Luther, O. Song, B. K. Hughes, C. L. Perkins, A. J. Nozik, *J. Am. Chem. Soc.* **2008**, *130*, 5974.

[8] M. S. Kang, J. Lee, D. J. Norris, C. D. Frisbie, *Nano Lett.* **2009**, *9*, 3848.

[9] A. G. Pattantyus-Abraham, I. J. Kramer, A. R. Barkhouse, X. Wang, G. Konstantatos, R. Debnath, L. Levina, I. Raabe, M. K. Nazeeruddin, M. Grätzel, E. H. Sargent, *ACS Nano* **2010**, *4*, 3374.

[10] W. K. Koh, S. R. Saudari, A. T. Fafarman, C. R. Kagan, C. B. Murray, *Nano Lett.* **2011**, *11*, 4764.

[11] J. Tang, K. W. Kemp, S. Hoogland, K. S. Jeong, H. Liu, L. Levina, M. Furukawa, X. Wang, R. Debnath, D. Cha, K. W. Chou, A. Fischer, A. Amassian, J. B. Asbury, E. H. Sargent, *Nat. Mater.* **2011**, *10*, 765.

[12] A. H. Ip, S. M. Thon, S. Hoogland, O. Voznyy, D. Zhitomirsky, R. Debnath, L. Levina, L. R. Rollny, G. H. Carey, A. Fischer, K. W. Kemp, I. J. Kramer, Z. Ning, A. J. Labelle, K. W. Chou, A. Amassian, E. H. Sargent, *Nat. Nanotechnol.* **2012**, *7*, 577.

[13] D. Zhitomirsky, M. Furukawa, J. Tang, P. Stadler, S. Hoogland, O. Voznyy, H. Liu, E. H. Sargent, *Adv. Mater.* **2012**, *24*, 6181.

[14] Y. Liu, J. Tolentino, M. Gibbs, R. Ihly, C. L. Perkins, Y. Liu, N. Crawford, J. C. Hemminger, M. Law, *Nano Lett.* **2013**, *13*, 1578.

[15] S. Z. Bisri, C. Piliego, M. Yarema, W. Heiss, M. A. Loi, *Adv. Mater.* **2013**, *25*, 4309.

[16] C. R. Kagan, C. B. Murray, *Nat. Nanotechnol.* **2015**, *10*, 1013.

[17] C. R. Kagan, E. Lifshitz, E. H. Sargent, D. V. Talapin, *Science* **2016**, *353*, 885.

[18] J. Jang, D. S. Dolzhnikov, W. Liu, S. Nam, M. Shim, D. V. Talapin, *Nano Lett.* **2015**, *15*, 6309.

[19] M. Liu, O. Voznyy, R. Sabatini, G. De Arquer, F. Pelayo, R. Munir, A. H. Balawi, X. Lan, F. Fan, G. Walters, A. R. Kirmani, S. Hoogland, F. Laquai, A. Amassian, E. H. Sargent, *Nat. Mater.* **2017**, *16*, 258.

[20] A. G. Shulga, V. Derenskyi, J. M. Salazar Rios, D. N. Dirin, M. Fritsch, M. V. Kovalenko, U. Scherf, M. A. Loi, *Adv. Mater.* **2017**, *29*, 1701764.

[21] D. M. Balazs, D. N. Dirin, H. Fang, L. Protesescu, G. H. ten Brink, B. J. Kooi, M. V. Kovalenko, M. A. Loi, *ACS Nano* **2015**, *9*, 11951.

[22] M. V. Kovalenko, M. Scheele, D. V. Talapin, *Science* **2009**, *324*, 1417.

[23] R. Tangirala, J. Baker, A. P. Alivisatos, D. Milliron, *Angew. Chem., Int. Ed.* **2010**, *49*, 2878.

[24] M. V. Kovalenko, M. I. Bodnarchuk, J. Zaumseil, J. S. Lee, D. V. Talapin, *J. Am. Chem. Soc.* **2010**, *132*, 10085.

[25] A. Nag, M. V. Kovalenko, J. Lee, W. Liu, B. Spokoyny, D. V. Talapin, *J. Am. Chem. Soc.* **2011**, *133*, 10612.

[26] A. T. Fafarman, W. K. Koh, B. T. Diroll, D. K. Kim, D. K. Ko, S. J. Oh, X. Ye, V. Doan-Nguyen, M. R. Crump, D. C. Reifsnyder, C. B. Murray, C. R. Kagan, *J. Am. Chem. Soc.* **2011**, *133*, 15753.

[27] S. Yakunin, D. N. Dirin, L. Protesescu, M. Sytnyk, S. Tollabimazraehno, M. Humer, F. Hackl, T. Fromherz, M. I. Bodnarchuk, M. V. Kovalenko, W. Heiss, *ACS Nano* **2014**, *8*, 12883.

[28] M. V. Kovalenko, R. D. Schaller, D. Jarzab, M. A. Loi, D. V. Talapin, *J. Am. Chem. Soc.* **2012**, *134*, 2457.

[29] D. S. Dolzhnikov, H. Zhang, J. Jaeyoung, J. S. Son, M. G. Panthani, T. Shibata, S. Chattopadhyay, D. V. Talapin, *Science* **2015**, *347*, 425.

[30] J. Choi, A. T. Fafarman, S. J. Oh, D. Ko, D. K. Kim, B. T. Diroll, S. Muramoto, J. G. Gillen, C. B. Murray, C. R. Kagan, *Nano Lett.* **2012**, *12*, 2631.

**ADVANCED
SCIENCE NEWS**

www.advancedsciencenews.com

**ADVANCED
MATERIALS**

www.advmat.de

[31] D. Tsokkou, P. Papagiorgis, L. Protesescu, M. V. Kovalenko, S. A. Choulis, C. Christofides, G. Itskos, A. Othonos, *Adv. Energy Mater.* **2014**, *4*, 1301547.

[32] C. Giansante, L. Carbone, C. Giannini, D. Altamura, Z. Ameer, G. Maruccio, A. Loiudice, M. R. Belviso, P. D. Cozzoli, A. Rizzo, G. Gigli, *J. Phys. Chem. C* **2013**, *117*, 13305.

[33] A. Fischer, L. Rollny, J. Pan, G. H. Carey, S. M. Thon, S. Hoogland, O. Voznyy, D. Zhitomirsky, J. Y. Kim, O. M. Bakr, E. H. Sargent, *Adv. Mater.* **2013**, *25*, 5742.

[34] C. C. Reinhart, E. Johansson, *J. Am. Chem. Soc.* **2017**, *139*, 5827.

[35] C. H. Chuang, P. R. Brown, V. Bulovic, M. G. Bawendi, *Nat. Mater.* **2014**, *13*, 796.

[36] Z. Ning, O. Voznyy, J. Pan, S. Hoogland, V. Adinolfi, J. Xu, M. Li, A. R. Kirmani, J. Sun, J. Minor, K. W. Kemp, H. Dong, L. Rollny, A. Labelle, G. Carey, B. Sutherland, I. Hill, A. Amassian, H. Liu, J. Tang, O. M. Bakr, E. H. Sargent, *Nat. Mater.* **2014**, *13*, 822.

[37] D. N. Dirin, S. Dreyfuss, M. I. Bodnarchuk, G. Nedelcu, P. Papagiorgis, G. Itskos, M. V. Kovalenko, *J. Am. Chem. Soc.* **2014**, *136*, 6550.

[38] H. Zhang, J. Jang, W. Liu, D. V. Talapin, *ACS Nano* **2014**, *8*, 7359.

[39] S. Kim, J. Noh, H. Choi, H. Ha, J. H. Song, H. C. Shim, J. Jang, M. C. Beard, S. Jeong, *J. Phys. Chem. Lett.* **2014**, *5*, 4002.

[40] H. Zhang, K. Dasbiswas, N. B. Ludwig, G. Han, B. Lee, S. Vaikuntanathan, D. V. Talapin, *Nature* **2017**, *542*, 328.

[41] H. Fang, R. Raissa, M. Abdu-Aguye, S. Adjokatse, G. R. Blake, J. Even, M. A. Loi, *Adv. Funct. Mater.* **2015**, *25*, 2378.

[42] Z. Yang, E. Yassitepe, O. Voznyy, A. Janmohamed, X. Lan, L. Levina, R. Comin, E. H. Sargent, *J. Am. Chem. Soc.* **2015**, *137*, 14869.

[43] M. Sytnyk, S. Yakunin, W. Schöfberger, R. T. Lechner, M. Burian, L. Ludescher, N. A. Killilea, A. Yousefi Amin, D. Kriegner, J. Stangl, H. Groiss, W. Heiss, *ACS Nano* **2017**, *11*, 1246.

[44] Z. Ning, X. Gong, R. Comin, G. Walters, F. Fan, O. Voznyy, E. Yassitepe, A. Buin, S. Hoogland, E. H. Sargent, *Nature* **2015**, *523*, 324.

[45] Q. Lin, H. J. Yun, W. Liu, H. Song, N. S. Makarov, O. Isaienko, T. Nakotte, G. Chen, H. Luo, V. I. Klimov, J. M. Pietryga, *J. Am. Chem. Soc.* **2017**, *139*, 6644.

[46] H. Choi, J. Ko, Y. Kim, S. Jeong, *J. Am. Chem. Soc.* **2013**, *135*, 5278.

[47] C. Fang, M. A. van Huis, D. Vanmaekelbergh, H. W. Zandbergen, *ACS Nano* **2010**, *4*, 211.

[48] D. Zherebetskyy, M. Scheele, Y. Zhang, N. Bronstein, C. Thompson, D. Britt, M. Salmeron, P. Alivisatos, L. W. Wang, *Science* **2014**, *344*, 1380.

[49] Z. Ning, H. Dong, Q. Zhang, O. Voznyy, E. H. Sargent, *ACS Nano* **2014**, *8*, 10321.

[50] A. Kiani, B. R. Sutherland, Y. Kim, O. Ouellette, L. Levina, G. Walters, C. Dinh, M. Liu, O. Voznyy, X. Lan, A. J. Labelle, A. H. Ip, A. Proppe, G. H. Ahmed, O. F. Mohammed, S. Hoogland, E. H. Sargent, *Appl. Phys. Lett.* **2016**, *109*, 183105.

[51] C. B. Murray, C. R. Kagan, M. G. Bawendi, *Science* **1995**, *270*, 1335.

[52] J. J. Choi, C. R. Bealing, K. Bian, K. J. Hughes, W. Zhang, D. Smilgies, R. G. Hennig, J. R. Engstrom, T. Hanrath, *J. Am. Chem. Soc.* **2011**, *133*, 3131.

[53] P. Simon, E. Rosseeva, I. A. Baburin, L. Liebscher, S. G. Hickey, R. Cardoso-Gil, A. Eychmüller, R. Kniep, W. Carrillo-Cabrera, *Angew. Chem., Int. Ed.* **2012**, *51*, 10776.

[54] P. Simon, L. Bahrig, I. A. Baburin, P. Formanek, F. Röder, J. Sickmann, S. G. Hickey, A. Eychmüller, H. Lichte, R. Kniep, E. Rosseeva, *Adv. Mater.* **2014**, *26*, 3042.

[55] S. J. Oh, N. E. Berry, J. H. Choi, E. A. Gaulding, H. Lin, T. Paik, B. T. Diroll, S. Muramoto, C. B. Murray, C. R. Kagan, *Nano Lett.* **2014**, *14*, 1559.

[56] W. J. Baumgardner, K. Whitham, T. Hanrath, *Nano Lett.* **2013**, *13*, 3225.

[57] T. Hanrath, D. Veldman, J. J. Choi, C. G. Christova, M. M. Wienk, R. A. J. Janssen, *ACS Appl. Mater. Interfaces* **2009**, *1*, 244.

[58] N. C. Anderson, M. P. Hendricks, J. J. Choi, J. S. Owen, *J. Am. Chem. Soc.* **2013**, *135*, 18536.

[59] C. S. S. Sandeep, J. M. Azpiroz, W. H. Evers, S. C. Boehme, I. Moreels, S. Kinge, L. D. A. Siebbeles, I. Infante, A. J. Houtepen, *ACS Nano* **2014**, *8*, 11499.

[60] A. Dong, J. Chen, P. M. Vora, J. M. Kikkawa, C. B. Murray, *Nature* **2010**, *466*, 474.

[61] W. H. Evers, B. Goris, S. Bals, M. Casavola, J. de Graaf, R. van Roij, M. Dijkstra, D. Vanmaekelbergh, *Nano Lett.* **2013**, *13*, 2317.

[62] A. Dong, Y. Jiao, D. J. Milliron, *ACS Nano* **2013**, *7*, 10978.

[63] R. Sharma, A. M. Sawvel, B. Barton, A. G. Dong, R. Buonsanti, A. Llordes, E. Schaible, S. Axnanda, Z. Liu, J. J. Urban, D. Nordlund, C. Kisielowski, D. J. Milliron, *Chem. Mater.* **2015**, *27*, 2755.

[64] W. Walravens, J. De Roo, E. Drijvers, S. Ten Brinck, E. Solano, J. Dendooven, C. Detavernier, I. Infante, Z. Hens, *ACS Nano* **2016**, *10*, 6861.

[65] M. Zhao, F. Yang, C. Liang, D. Wang, D. Ding, J. Lv, J. Zhang, W. Hu, C. Lu, Z. Tang, *Adv. Funct. Mater.* **2016**, *26*, 5182.

[66] M. Alimoradi Jazi, V. A. E. C. Janssen, W. H. Evers, A. Tadjine, C. Delerue, L. D. A. Siebbeles, H. S. J. van der Zant, A. J. Houtepen, D. Vanmaekelbergh, *Nano Lett.* **2017**, *17*, 5238.

[67] D. M. Balazs, *PhD Thesis*, University of Groningen, **2018**

[68] K. Whitham, T. Hanrath, *J. Phys. Chem. Lett.* **2017**, *8*, 2623.

[69] D. Li, M. H. Nielsen, J. R. Lee, C. Frandsen, J. F. Banfield, J. J. De Yoreo, *Science* **2012**, *336*, 1014.

[70] J. J. Geuchies, C. Van Overbeek, W. H. Evers, B. Goris, A. De Backer, A. P. Gantapara, F. T. Rabouw, J. Hilhorst, J. L. Peters, O. Konovalov, A. V. Petukhov, M. Dijkstra, L. D. A. Siebbeles, S. Van Aert, S. Bals, D. Vanmaekelbergh, *Nat. Mater.* **2016**, *15*, 1248.

[71] D. Smilgies, T. Hanrath, *EPL* **2017**, *119*, 28003.

[72] W. H. Evers, J. M. Schins, M. Aerts, A. Kulkarni, P. Capiod, M. Berthe, B. Grandidier, C. Delerue, H. S. J. van der Zant, C. v. Overbeek, J. L. Peters, D. Vanmaekelbergh, L. D. A. Siebbeles, *Nat. Commun.* **2015**, *6*, 9195.

[73] M. C. Weidman, D. M. Smilgies, W. A. Tisdale, *Nat. Mater.* **2016**, *15*, 775.

[74] M. P. Boneschanscher, W. H. Evers, J. J. Geuchies, T. Altantzis, B. Goris, F. T. Rabouw, S. A. van Rossum, H. S. van der Zant, L. D. Siebbeles, G. Van Tendeloo, I. Swart, J. Hilhorst, A. V. Petukhov, S. Bals, D. Vanmaekelbergh, *Science* **2014**, *344*, 1377.

[75] P. Guyot-Sionnest, *J. Phys. Chem. Lett.* **2012**, *3*, 1169.

[76] M. Scheele, *Z. Phys. Chem.* **2015**, *229*, 167.

[77] C. P. Collier, R. J. Saykally, J. J. Shiang, S. E. Henrichs, J. R. Heath, *Science* **1997**, *277*, 1978.

[78] M. C. Weidman, M. E. Beck, R. S. Hoffman, F. Prins, W. A. Tisdale, *ACS Nano* **2014**, *8*, 6363.

[79] I. Moreels, K. Lambert, D. Smeets, D. De Muynck, T. Nollet, J. C. Martins, F. Vanhaecke, A. Vantomme, C. Delerue, G. Allan, Z. Hens, *ACS Nano* **2009**, *3*, 3023.

[80] R. H. Gilmore, E. M. Y. Lee, M. C. Weidman, A. P. Willard, W. A. Tisdale, *Nano Lett.* **2017**, *17*, 893.

[81] I. Chu, M. Radulaski, N. Vukmirovic, H. Cheng, L. Wang, *J. Phys. Chem. C* **2011**, *115*, 21409.

[82] R. A. Marcus, *J. Chem. Phys.* **1956**, *24*, 966.

[83] N. Prodanovic, N. Vukmirovic, Z. Ikonic, P. Harrison, D. Indjin, *J. Phys. Chem. Lett.* **2014**, *5*, 1335.

[84] J. R. Miller, L. T. Calcaterra, G. L. Closs, *J. Am. Chem. Soc.* **1984**, *106*, 3047.

[85] D. W. Koon, T. G. Castner, *Solid State Commun.* **1987**, *64*, 11.

[86] S. Wang, M. Ha, M. Manno, C. D. Frisbie, C. Leighton, *Nat. Commun.* **2012**, *3*, 2213.

[87] K. Kang, S. Watanabe, K. Broch, A. Sepe, A. Brown, I. Nasrallah, M. Nikolka, Z. Fei, M. Heeney, D. Matsumoto, K. Marumoto, H. Tanaka, S. Kuroda, H. Sirringhaus, *Nat. Mater.* **2016**, *15*, 896.

[88] L. Friedman, T. Holstein, *Ann. Phys.* **1963**, *21*, 494.

[89] K. Whitham, J. Yang, B. H. Savitzky, L. F. Kourkoutis, F. Wise, T. Hanrath, *Nat. Mater.* **2016**, *15*, 557.

[90] E. J. D. Klem, H. Shukla, S. Hinds, D. D. MacNeil, L. Levina, E. H. Sargent, *Appl. Phys. Lett.* **2008**, *92*, 212105.

[91] D. M. Balazs, M. I. Nugraha, S. Z. Bisri, M. Sytnyk, W. Heiss, M. A. Loi, *Appl. Phys. Lett.* **2014**, *104*, 112104.

[92] A. Hassinen, I. Moreels, K. De Nolf, P. F. Smet, J. C. Martins, Z. Hens, *J. Am. Chem. Soc.* **2012**, *134*, 20705.

[93] A. R. Kirmani, G. H. Carey, M. Abdelsamie, B. Yan, D. Cha, L. R. Rollny, X. Cui, E. H. Sargent, A. Amassian, *Adv. Mater.* **2014**, *26*, 4717.

[94] A. M. Schimpf, K. E. Knowles, G. M. Carroll, D. R. Gamelin, *Acc. Chem. Res.* **2015**, *48*, 1929.

[95] R. Gresback, N. J. Kramer, Y. Ding, T. Chen, U. R. Kortshagen, T. Nozaki, *ACS Nano* **2014**, *8*, 5650.

[96] A. Stavrinadis, G. Konstantatos, *ChemPhysChem* **2016**, *17*, 632.

[97] A. Sahu, M. S. Kang, A. Kompch, C. Notthoff, A. W. Wills, D. Deng, M. Winterer, C. D. Frisbie, D. J. Norris, *Nano Lett.* **2012**, *12*, 2587.

[98] D. M. Kroupa, B. K. Hughes, E. M. Miller, D. T. Moore, N. C. Anderson, B. D. Chernomordik, A. J. Nozik, M. C. Beard, *J. Am. Chem. Soc.* **2017**, *139*, 10382.

[99] M. Soreni-Hararl, N. Yaacobi-Gross, D. Steiner, A. Aharoni, U. Banin, O. Millo, N. Tessler, *Nano Lett.* **2008**, *8*, 678.

[100] N. Yaacobi-Gross, M. Soreni-Harari, M. Zimin, S. Kababya, A. Schmidt, N. Tessler, *Nat. Mater.* **2011**, *10*, 974.

[101] D. M. Kroupa, M. Vörös, N. P. Brawand, B. W. McNichols, E. M. Miller, J. Gu, A. J. Nozik, A. Sellinger, G. Galli, M. C. Beard, *Nat. Commun.* **2017**, *8*, 15257.

[102] P. R. Brown, D. Kim, R. R. Lunt, N. Zhao, M. G. Bawendi, J. C. Grossman, V. Bulovic, *ACS Nano* **2014**, *8*, 5863.

[103] W. Koh, A. Y. Koposov, J. T. Stewart, B. N. Pal, I. Robel, J. M. Pietryga, V. I. Klimov, *Sci. Rep.* **2013**, *3*, 2004.

[104] R. N. Pereira, J. Coutinho, S. Niesar, T. A. Oliveira, W. Aigner, H. Wiggers, M. J. Rayson, P. R. Briddon, M. S. Brandt, M. Stutzmann, *Nano Lett.* **2014**, *14*, 3817.

[105] A. R. Kirmani, A. Kiani, M. M. Said, O. Voznyy, N. Wehbe, G. Walters, S. Barlow, E. H. Sargent, S. R. Marder, A. Amassian, *ACS Energy Lett.* **2016**, *1*, 922.

[106] M. I. Nugraha, S. Kumagai, S. Watanabe, M. Sytnyk, W. Heiss, M. A. Loi, J. Takeya, *ACS Appl. Mater. Interfaces* **2017**, *9*, 18039.

[107] A. R. Kirmani, F. Pelayo García de Arquer, J. Z. Fan, J. I. Khan, G. Walters, S. Hoogland, N. Wehbe, M. M. Said, S. Barlow, F. Laquai, S. R. Marder, E. H. Sargent, A. Amassian, *ACS Energy Lett.* **2017**, *2*, 1952.

[108] M. Scheele, D. Hanifi, D. Zherebetskyy, S. T. Chourou, S. Axnanda, B. J. Rancatore, K. Thorkelsson, T. Xu, Z. Liu, L. Wang, Y. Liu, A. P. Alivisatos, *ACS Nano* **2014**, *8*, 2532.

[109] C. Giansante, I. Infante, E. Fabiano, R. Grisorio, G. P. Suranna, G. Gigli, *J. Am. Chem. Soc.* **2015**, *137*, 1875.

[110] D. M. Kroupa, N. C. Anderson, C. V. Castaneda, A. J. Nozik, M. C. Beard, *Chem. Commun.* **2016**, *52*, 13893.

[111] H. Lu, J. Joy, R. L. Gaspar, S. E. Bradforth, R. L. Brutchey, *Chem. Mater.* **2016**, *28*, 1897.

[112] V. Sayevich, C. Guhrenz, M. Sin, V. M. Dzhagan, A. Weiz, D. Kasemann, E. Brunner, M. Ruck, D. R. T. Zahn, K. Leo, N. Gaponik, A. Eychmüller, *Adv. Funct. Mater.* **2016**, *26*, 2163.

[113] D. Debellis, G. Gigli, S. ten Brinck, I. Infante, C. Giansante, *Nano Lett.* **2017**, *17*, 1248.

[114] D. M. Balazs, K. I. Bijlsma, H. Fang, D. N. Dirin, M. Döbeli, M. V. Kovalenko, M. A. Loi, *Sci. Adv.* **2017**, *3*, eaao1558.

[115] Y. Bekenstein, K. Vinokurov, S. Keren-Zur, I. Hadar, Y. Schilt, U. Raviv, O. Millo, U. Banin, *Nano Lett.* **2014**, *14*, 1349.

[116] J. D. Forster, J. J. Lynch, N. E. Coates, J. Liu, H. Jang, E. Zaia, M. P. Gordon, M. Szybowski, A. Sahu, D. G. Cahill, J. J. Urban, *Sci. Rep.* **2017**, *7*, 2765.

[117] S. J. Oh, N. E. Berry, J. Choi, E. A. Gaulding, T. Paik, S. Hong, C. B. Murray, C. R. Kagan, *ACS Nano* **2013**, *7*, 2413.

[118] E. L. Rosen, A. M. Sawvel, D. J. Milliron, B. A. Helms, *Chem. Mater.* **2014**, *26*, 2214.

[119] D. Kim, D. Kim, J. Lee, J. C. Grossman, *Phys. Rev. Lett.* **2013**, *110*, 196802.

[120] D. K. Kim, A. T. Fafarman, B. T. Diroll, S. H. Chan, T. R. Gordon, C. B. Murray, C. R. Kagan, *ACS Nano* **2013**, *7*, 8760.

[121] B. E. Treml, B. H. Savitzky, A. M. Tirmzi, J. C. DaSilva, L. F. Kourkoutis, T. Hanrath, *ACS Appl. Mater. Interfaces* **2017**, *9*, 13500.

[122] D. A. R. Barkhouse, R. Debnath, I. J. Kramer, D. Zhitomirsky, A. G. Pattantyus-Abraham, L. Levina, L. Etgar, M. Grätzel, E. H. Sargent, *Adv. Mater.* **2011**, *23*, 3134.

[123] C. Piliego, L. Protesescu, S. Z. Bisri, M. V. Kovalenko, M. A. Loi, *Energy Environ. Sci.* **2013**, *6*, 3054.

[124] Z. Yang, A. Janmohamed, X. Lan, F. Pelayo García de Arquer, O. Voznyy, E. Yassitepe, G. Kim, Z. Ning, X. Gong, R. Comin, E. H. Sargent, *Nano Lett.* **2015**, *15*, 7539.

[125] Z. Yang, J. Z. Fan, A. H. Proppe, F. Pelayo García de Arquer, D. Rossouw, O. Voznyy, X. Lan, M. Liu, G. Walters, R. Quintero-Bermudez, B. Sun, S. Hoogland, G. A. Botton, S. O. Kelley, E. H. Sargent, *Nat. Commun.* **2017**, *8*, 1325.

[126] H. Aqoma, M. Al Mubarok, W. T. Hadmojo, E. Lee, T. Kim, T. K. Ahn, S. Oh, S. Jang, *Adv. Mater.* **2017**, *29*, 1605756.

[127] M. J. Speirs, D. M. Balazs, D. N. Dirin, M. V. Kovalenko, M. A. Loi, *Appl. Phys. Lett.* **2017**, *110*, 103904.

[128] M. J. Speirs, D. N. Dirin, M. Abdu-Aguye, D. M. Balazs, M. V. Kovalenko, M. A. Loi, *Energy Environ. Sci.* **2016**, *9*, 2916.

[129] J. Lee, M. V. Kovalenko, J. Huang, D. S. Chung, D. V. Talapin, *Nat. Nanotechnol.* **2011**, *6*, 348.

[130] A. Nag, D. S. Chung, D. S. Dolzhnikov, N. M. Dimitrijevic, S. Chattopadhyay, T. Shibata, D. V. Talapin, *J. Am. Chem. Soc.* **2012**, *134*, 13604.

[131] J. H. Choi, H. Wang, S. J. Oh, T. Paik, P. Sung, J. Sung, X. Ye, T. Zhao, B. T. Diroll, C. B. Murray, C. R. Kagan, *Science* **2016**, *352*, 205.

[132] V. Sayevich, N. Gaponik, M. Plötner, M. Kruszynska, T. Gemming, V. M. Dzhagan, S. Akhavan, D. R. T. Zahn, H. V. Demir, A. Eychmüller, *Chem. Mater.* **2015**, *27*, 4328.

[133] D. M. Balazs, N. Rizkia, H. Fang, D. N. Dirin, J. Momand, B. J. Kooi, M. V. Kovalenko, M. A. Loi, *ACS Appl. Mater. Interfaces* **2018**, *10*, 5626

[134] C. H. Jo, J. H. Kim, J. Kim, J. Kim, M. S. Oh, M. S. Kang, M. Kim, Y. Kim, B. Ju, S. K. Park, *J. Mater. Chem. C* **2014**, *2*, 10305.

[135] D. S. Chung, J. S. Lee, J. Huang, A. Nag, S. Ithurria, D. V. Talapin, *Nano Lett.* **2012**, *12*, 1813.

[136] D. K. Kim, Y. Lai, B. T. Diroll, C. B. Murray, C. R. Kagan, *Nat. Commun.* **2012**, *3*, 1216.

[137] S. J. Oh, Z. Wang, N. E. Berry, J. H. Choi, T. Zhao, E. A. Gaulding, T. Paik, Y. Lai, C. B. Murray, C. R. Kagan, *Nano Lett.* **2014**, *14*, 6210.

[138] V. Derenskyi, W. Gomulya, J. M. S. Rios, M. Fritsch, N. Fröhlich, S. Jung, S. Allard, S. Z. Bisri, P. Gordiichuk, A. Herrmann, U. Scherf, M. A. Loi, *Adv. Mater.* **2014**, *26*, 5969.

[139] J. Schornbaum, Y. Zakharko, M. Held, S. Thiemann, F. Gannott, J. Zaumseil, *Nano Lett.* **2015**, *15*, 1822.

[140] S. Z. Bisri, S. Shimizu, M. Nakano, Y. Iwasa, *Adv. Mater.* **2017**, *29*, 1607054.

1800082 (14 of 15)

[141] C. Wang, M. Shim, P. Guyot-Sionnest, *Science* **2001**, *291*, 2390.

[142] D. Yu, C. Wang, P. Guyot-Sionnest, *Science* **2003**, *300*, 1277.

[143] H. Liu, A. Pourret, P. Guyot-Sionnest, *ACS Nano* **2010**, *4*, 5211.

[144] S. Z. Bisri, E. Degoli, N. Spallanzani, G. Krishnan, B. J. Kooi, C. Ghica, M. Yarema, W. Heiss, O. Pulci, S. Ossicini, M. A. Loi, *Adv. Mater.* **2014**, *26*, 5639.

[145] H. Heo, M. H. Lee, J. Yang, H. S. Wee, J. Lim, D. Hahm, J. W. Yu, W. K. Bae, W. B. Lee, M. S. Kang, K. Char, *Nano Lett.* **2017**, *17*, 2433.

[146] M. I. Nugraha, H. Matsui, S. Watanabe, T. Kubo, R. Häusermann, S. Z. Bisri, M. Sytnyk, W. Heiss, M. A. Loi, J. Takeya, *Adv. Electron. Mater.* **2017**, *3*, 1600360.

[147] E. S. Toberer, G. J. Snyder, *Nat. Mater.* **2008**, *7*, 105.

[148] C. J. Vineis, A. Shakouri, A. Majumdar, M. G. Kanatzidis, *Adv. Mater.* **2010**, *22*, 3970.

[149] M. Ibáñez, R. J. Korkosz, Z. Luo, P. Riba, D. Cadavid, S. Ortega, A. Cabot, M. G. Kanatzidis, *J. Am. Chem. Soc.* **2015**, *137*, 4046.

[150] M. Ibáñez, R. Hasler, Y. Liu, O. Dobrozhan, O. Nazarenko, D. Cadavid, A. Cabot, M. V. Kovalenko, *Chem. Mater.* **2017**, *29*, 7093.

[151] M. Ibáñez, Z. Luo, A. Genç, L. Piveteau, S. Ortega, D. Cadavid, O. Dobrozhan, Y. Liu, M. Nachtegaal, M. Zebarjadi, J. Arbiol, M. V. Kovalenko, A. Cabot, *Nat. Commun.* **2016**, *7*, 10766.

[152] D. Ding, D. Wang, M. Zhao, J. Lv, H. Jiang, C. Lu, Z. Tang, *Adv. Mater.* **2017**, *29*, 1603444.

[153] L. D. Hicks, M. S. Dresselhaus, *Phys. Rev. B* **1993**, *47*, 12727.

[154] L. D. Hicks, M. S. Dresselhaus, *Phys. Rev. B* **1993**, *47*, 16631.

[155] T. C. Harman, P. J. Taylor, M. P. Walsh, B. E. LaForge, *Science* **2002**, *297*, 2229.

[156] J. J. Urban, *Nat. Nanotechnol.* **2015**, *10*, 997.

[157] W. Ong, S. M. Rupich, D. V. Talapin, A. J. H. McGaughey, J. A. Malen, *Nat. Mater.* **2013**, *12*, 410.

[158] R. Y. Wang, J. P. Feser, J. Lee, D. V. Talapin, R. Segalman, A. Majumdar, *Nano Lett.* **2008**, *8*, 2283.

[159] D. Ko, C. B. Murray, *ACS Nano* **2011**, *5*, 4810.

[160] J. Choi, K. Cho, J. Yun, Y. Park, S. Yang, S. Kim, *Adv. Energy Mater.* **2017**, *7*, 1700972.

[161] A. Kiani, H. Fayaz Movahed, S. Hoogland, O. Voznyy, R. Wolowiec, L. Levina, F. Pelayo Garcia de Arquer, P. Pietsch, X. Wang, P. Maraghechi, E. H. Sargent, *ACS Energy Lett.* **2016**, *1*, 740.

1800082 (15 of 15)